

OPEN

Direct, gabapentin-insensitive interaction of a soluble form of the calcium channel subunit $\alpha_2\delta$ -1 with thrombospondin-4

Ehab El-Awaad^{1,2}, Galya Prymachuk³, Cora Fried¹, Jan Matthes¹, Jörg Isensee⁴, Tim Hucho⁴, Wolfram F. Neiss³, Mats Paulsson^{5,6}, Stefan Herzig^{1,7}, Frank Zaucke^{5,8} & Markus Pietsch^{1*}

The $\alpha_2\delta$ -1 subunit of voltage-gated calcium channels binds to gabapentin and pregabalin, mediating the analgesic action of these drugs against neuropathic pain. Extracellular matrix proteins from the thrombospondin (TSP) family have been identified as ligands of $\alpha_2\delta$ -1 in the CNS. This interaction was found to be crucial for excitatory synaptogenesis and neuronal sensitisation which in turn can be inhibited by gabapentin, suggesting a potential role in the pathogenesis of neuropathic pain. Here, we provide information on the biochemical properties of the direct TSP/ $\alpha_2\delta$ -1 interaction using an ELISA-style ligand binding assay. Our data reveal that full-length pentameric TSP-4, but neither TSP-5/COMP of the pentamer-forming subgroup B nor TSP-2 of the trimer-forming subgroup A directly interact with a soluble variant of $\alpha_2\delta$ -1 ($\alpha_2\delta$ -1_s). Interestingly, this interaction is not inhibited by gabapentin on a molecular level and is not detectable on the surface of HEK293-EBNA cells over-expressing $\alpha_2\delta$ -1 protein. These results provide biochemical evidence that supports a specific role of TSP-4 among the TSPs in mediating the binding to neuronal $\alpha_2\delta$ -1 and suggest that gabapentin does not directly target TSP/ $\alpha_2\delta$ -1 interaction to alleviate neuropathic pain.

Thrombospondins (TSPs) form a family of five large oligomeric extracellular matrix glycoproteins that are expressed by numerous cell types, playing important roles in cellular migration, attachment and cytoskeletal dynamics^{1,2}. Several TSP isoforms have been shown to be involved in a variety of physiological and pathological processes, including regulation of angiogenesis, apoptosis and platelet aggregation³⁻⁵. TSPs can be subdivided into subgroups A (TSP-1 and 2) and B (TSP-3-5, with TSP-5 also referred to as cartilage oligomeric matrix protein (COMP)) based on their oligomerisation state (trimeric or pentameric, respectively) and domain structure (Fig. 1A). In neurons, astrocyte-secreted or recombinantly expressed TSP(s), particularly TSP-1, TSP-2 and TSP-4, were reported to promote the formation of excitatory synapses both *in vitro* and *in vivo* through interaction with the voltage-gated calcium channel subunit $\alpha_2\delta$ -1⁶⁻¹⁰. The $\alpha_2\delta$ proteins ($\alpha_2\delta$ -1-4) are auxiliary subunits of voltage-gated calcium channels Ca_v1 and Ca_v2 , and were found to be encoded by four different genes¹¹⁻¹³. Functions of these auxiliary subunits include the modulation of trafficking, expression in the plasma membrane¹⁴⁻¹⁷, and biophysical properties of the channels^{15,17-19}. Importantly, $\alpha_2\delta$ -1 acts as a specific binding site for gabapentinoid drugs^{20,21}, mediating their analgesic effect in neuropathic pain²¹⁻²³. Furthermore, studies using different animal models of neuropathic pain indicated the involvement of $\alpha_2\delta$ -1 in pain development, with nerve

¹Institute II for Pharmacology, Centre of Pharmacology, Medical Faculty, University of Cologne, Gleueler Str. 24, D-50931, Cologne, Germany. ²Department of Pharmacology, Faculty of Medicine, Assiut University, Assiut, 71515, Egypt. ³Department of Anatomy I, Medical Faculty, University of Cologne, Kerpener Str. 62, D-50937, Cologne, Germany. ⁴Experimental Anaesthesiology and Pain Research, Department of Anaesthesiology and Intensive Care Medicine, Medical Faculty, University of Cologne, Robert-Koch-Str. 10, D-50931, Cologne, Germany. ⁵Institute for Biochemistry II, Centre for Biochemistry, Medical Faculty, University of Cologne, Joseph-Stelzmann-Str. 52, D-50931, Cologne, Germany. ⁶Centre for Molecular Medicine Cologne (CMMC), University of Cologne, Robert-Koch-Str. 21, D-50931, Cologne, Germany. ⁷President of TH Köln, TH Köln (University of Applied Sciences), Claudiusstr. 1, D-50678, Cologne, Germany. ⁸Dr. Rolf M. Schwiete Research Unit for Osteoarthritis, Orthopedic University Hospital, Friedrichsheim gGmbH, Marienburgstr. 2, D-60528, Frankfurt/Main, Germany. *email: markus.pietsch@uk-koeln.de

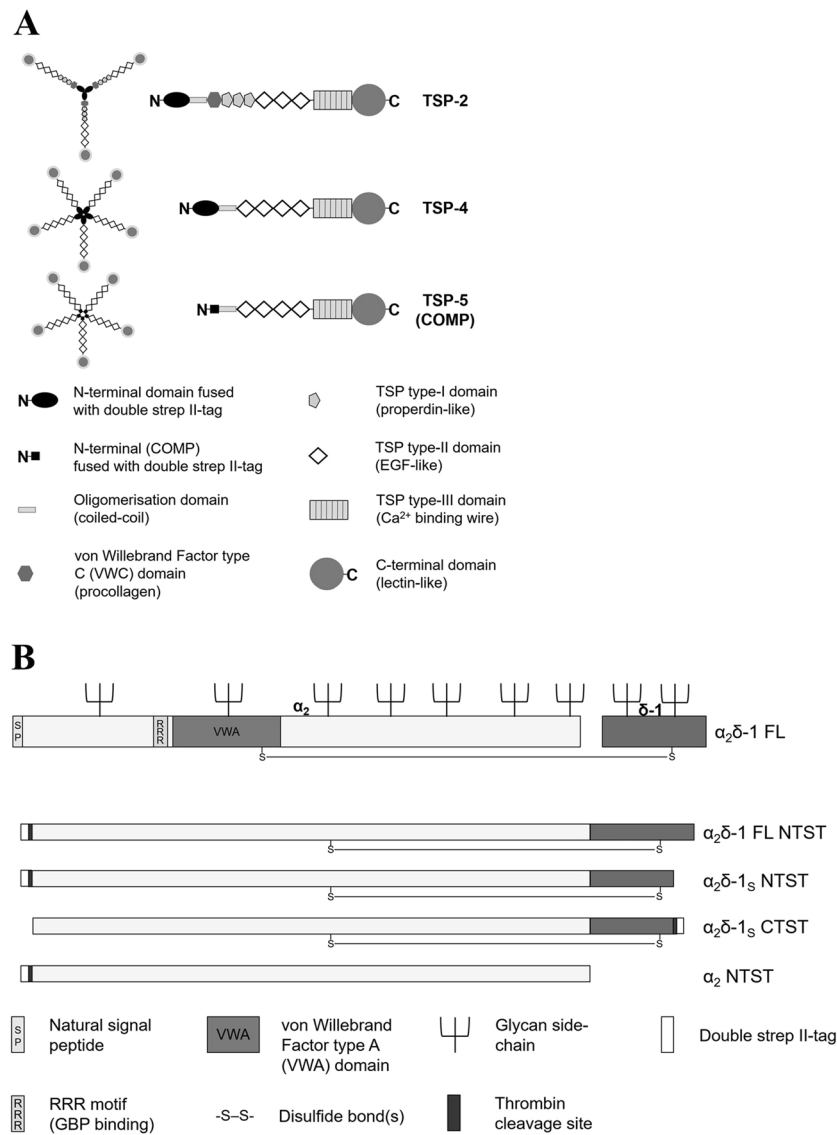


Figure 1. Schematic presentation of the structures of the recombinant proteins generated in this study. **(A)** Domain structure and oligomerisation state of the generated recombinant full-length TSP-2 (trimer), TSP-4 and COMP (pentamers). Schematic representation adapted by permission from Springer Nature, *Cell Mol Life Sci*, Structures of thrombospondins, Carlson, C. B., Lawler, J. & Mosher, D. F., Copyright (2008)³⁹. All recombinant TSPs have been expressed with an N-terminal double strep II-tag and contain glycan side-chains which are not shown for reasons of clarity. **(B)** Structure of $\alpha_2\delta-1$ FL protein (adapted from *Cell* 139, Eroglu, Ç. *et al.*, Gabapentin receptor $\alpha_2\delta-1$ is a neuronal thrombospondin receptor responsible for excitatory CNS synaptogenesis, 380–392, Copyright (2009), with permission from Elsevier⁷) and simplified depiction of the derived non-proteolytically processed $\alpha_2\delta-1$ mutants generated in this study. The RRR motif, the von Willebrand Factor type A domain, and the glycan side-chains are not shown in the $\alpha_2\delta-1$ mutants for reasons of clarity.

injuries leading to up-regulation of $\alpha_2\delta-1$ in both dorsal root ganglion (DRGs) and spinal dorsal horn neurons^{24–27} as well as to an increase of miniature excitatory post-synaptic current (mEPSC) frequency in the latter neurons^{22,25,26,28–30}. Similarly, injury-induced TSP-4 is reported to mediate central sensitisation and neuropathic pain states^{8,9,31–37}. This effect was recently shown to be mediated by activation of a TSP-4/ $\alpha_2\delta-1$ -dependent pathway which requires a direct molecular interaction between the two proteins^{9,34}. Furthermore, the presence of TSP-4 was shown to modestly but significantly reduce the binding affinity of ³H-gabapentin (³H-GBP) towards $\alpha_2\delta-1$ in membrane preparations from TSP-4/ $\alpha_2\delta-1$ co-transfected cells³⁸. Taken together, the TSP-4/ $\alpha_2\delta-1$ protein-protein interaction seems to be of potential translational importance and thus may serve as a novel target for developing a new class of analgesics against neuropathic pain.

The aim of the present study is to investigate the biochemical characteristics of the direct molecular interaction between TSPs and $\alpha_2\delta-1$, addressing the question whether $\alpha_2\delta-1$ binding is specific to TSP-4 or redundant among other TSPs. GBP has been shown so far to inhibit the interaction of $\alpha_2\delta-1$ with a truncated form of TSP-2

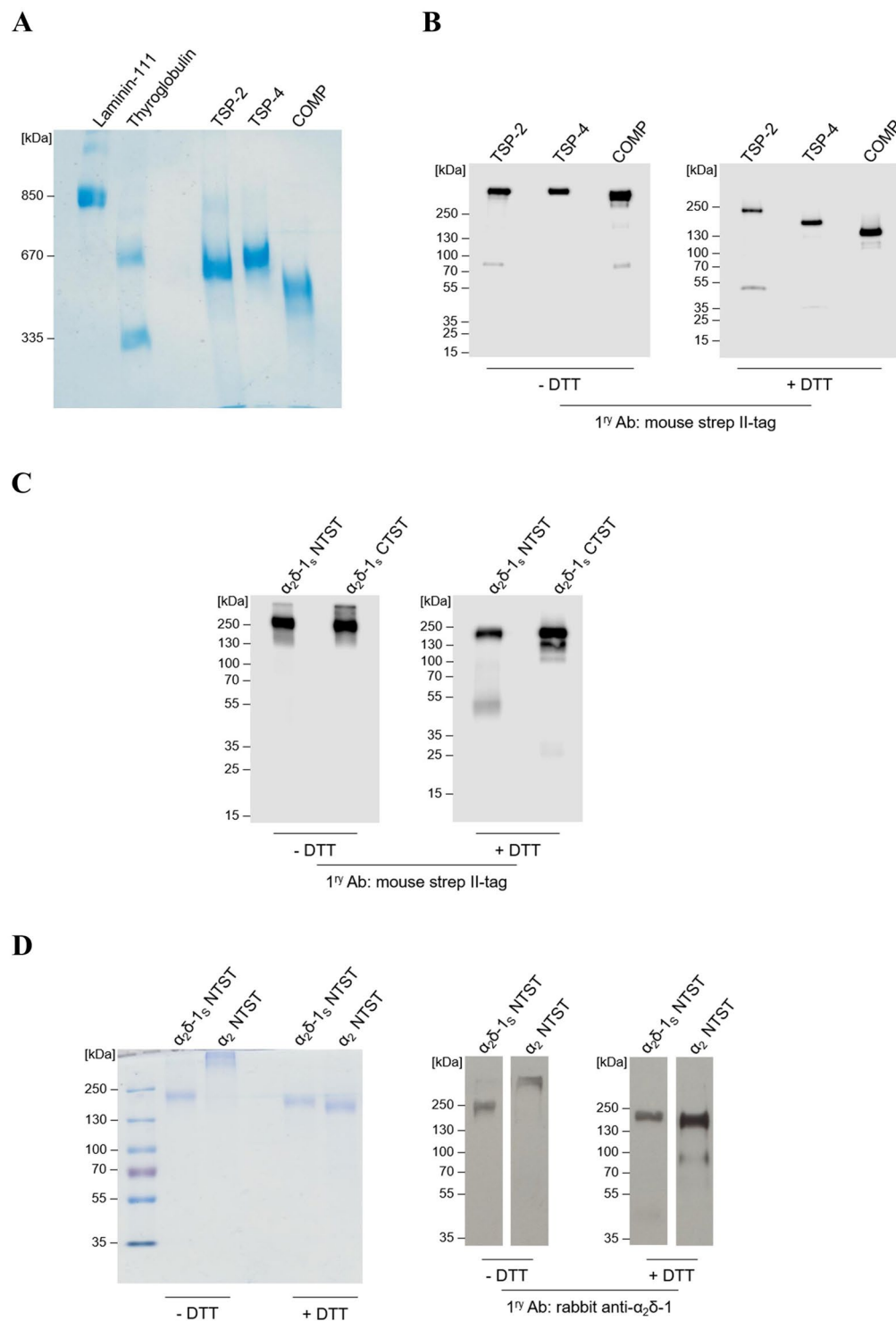


Figure 2. The generated recombinant TSPs and $\alpha_2\delta-1_S$ variants show high degree of purity and integrity in Coomassie staining and western blot analyses. (**A,D** left) Representative Coomassie-stained gels and (**B,C** and **D** right) immunoblots of three full-length TSP proteins, all carrying an N-terminal double strep II-tag: TSP-2, TSP-4, and COMP (**A,B**); $\alpha_2\delta-1_S$ variants carrying either an N-terminal ($\alpha_2\delta-1_S$ NTST) or a C-terminal ($\alpha_2\delta-1_S$ CTST) double strep II-tag (**C**); $\alpha_2\delta-1_S$ NTST and α_2 peptide chain carrying an N-terminal double strep II-tag, α_2 NTST (**D**). Proteins were separated under non-reducing (–DTT) or reducing conditions (+DTT) on 4–15% (**B**), 10% (**C**), and 7% (**D**) polyacrylamide gels, respectively, while in (**A**) proteins were separated on 0.5% agarose (w/v)/3% polyacrylamide (w/v) composite gels without prior DTT treatment. Proteins were either stained with colloidal Coomassie stain (**A,D** left) or detected with the following primary antibodies after blotting: mouse anti-strep II-tag (**B,C**) or rabbit anti- $\alpha_2\delta-1$ (**D** right). Secondary antibodies included the polyclonal rabbit anti-mouse IgG (**B,C**) and swine anti-rabbit IgG (**D** right), both conjugated with horseradish peroxidase (see Supplementary Table S2 for further information). In all gels the molecular weight standard

(in kDa) indicated on the left was PageRuler Plus Prestained Protein Ladder (Thermo Fisher Scientific) except for (A) in which both thyroglobulin (Sigma) and recombinant laminin-111 (kind gift from Prof. Dr. Monique Aumailley, Institute for Biochemistry II, Centre for Biochemistry, Medical Faculty, University of Cologne) were used.

in co-immunoprecipitation experiments⁷ as well as functionally by inhibiting synaptogenesis^{7,8,10}, neuron sensitisation and behavioural hypersensitivity induced by TSP-2, its truncated fragment and/or TSP-4^{9,34,35}. Thus, we examined whether the direct TSP/ $\alpha_2\delta$ -1 interaction can be inhibited by GBP on a molecular level as well. We therefore generated purified recombinant forms of three full-length TSPs (TSP-2, TSP-4 and COMP) as well as soluble forms of $\alpha_2\delta$ -1 subunit ($\alpha_2\delta$ -1_S), that shows GBP binding affinity similar to that of wild-type $\alpha_2\delta$ -1, and the α_2 peptide chain of $\alpha_2\delta$ -1 (Fig. 1). Both the interaction of these recombinant TSPs with $\alpha_2\delta$ -1 and the possible inhibition by GBP were examined in a solid-phase ELISA-style ligand binding assay, with the capability of soluble $\alpha_2\delta$ -1 to interact with GBP being proven by a newly developed surface plasmon resonance (SPR)-based binding assay. In order to demonstrate the characteristics of the direct TSP-4/ $\alpha_2\delta$ -1 interaction in an environment similar to that of native cells, we attempted to visualise the interaction of fluorescently labelled TSP-4 with membrane-localised full-length (FL) $\alpha_2\delta$ -1 in a cell-based system.

Results

Biochemical characteristics of recombinant purified proteins expressed in HEK293-EBNA cells. To investigate the direct binding of different TSPs to $\alpha_2\delta$ -1, three full-length recombinant TSPs, namely, the trimeric TSP-2, the pentameric proteins TSP-4 and COMP, and a soluble C-terminal deletion mutant of $\alpha_2\delta$ -1 carrying an N-terminal ($\alpha_2\delta$ -1_S NTST) or a C-terminal ($\alpha_2\delta$ -1_S CTST) double strep II-tag (Fig. 1) were generated in a eukaryotic expression system. Coomassie stained gels and immunoblots of the purified proteins confirmed their purity, identity and integrity (Fig. 2; Supplementary Fig. S1). As expected for TSPs, the intact proteins showed high molecular weight bands with approximate apparent molecular weights (M_r) in the range ~500–670 kDa when compared to laminin-111 and thyroglobulin as marker proteins (Fig. 2A). The oligomerisation patterns of these high molecular weight TSPs (*i.e.* pentamers for TSP-4 and COMP and trimer for TSP-2) were confirmed by comparing immunoblots in the absence and presence of the reducing reagent DTT (Fig. 2B; Supplementary Fig. S1a). In the latter case, DTT reduces the interchain disulphide bonds within the oligomerisation domains of the analysed TSPs³⁹ and major bands of monomeric proteins with M_r of TSP-2 (~240 kDa), TSP-4 (~160 kDa), and COMP (~130 kDa) were observed (Fig. 2B, +DTT; Supplementary Fig. S1a, +DTT).

Similar analysis was performed for the generated $\alpha_2\delta$ -1_S NTST and the respective C-terminally tagged $\alpha_2\delta$ -1 variant, $\alpha_2\delta$ -1_S CTST, showing single but smeared bands at approximate M_r ~200 kDa under non-reducing conditions (Fig. 2C, –DTT; Supplementary Fig. S1b, –DTT) and appear as distinct bands at approximate M_r ~180 kDa under reducing conditions (Fig. 2C, +DTT; Supplementary Fig. S1b, +DTT). So far, there is no comprehensive explanation for this gel band shift in the presence of DTT. However, it cannot be attributed to the reductive cleavage of the interchain disulphide bridge between α_2 and δ -1 followed by loss of the smaller δ -1 chain. This conclusion arises from the observation that $\alpha_2\delta$ -1_S bearing the C-terminal double strep II-tag ($\alpha_2\delta$ -1_S CTST) is still detectable in immunoblots probed with strep II-tag antibody following DTT treatment. In agreement with this result, mass spectra of $\alpha_2\delta$ -1_S NTST recorded with and without DTT pre-treatment showed almost identical molecular ion peaks ($[M + H]^+$; Table 1, Supplementary Fig. S2d,e). This observation confirms the results by Brown and Gee⁴⁰ who first described a similar soluble mutant of the porcine $\alpha_2\delta$ -1 orthologue which retains high affinity for ³H-GBP. Although uncleaved $\alpha_2\delta$ -1 may not represent a functional form as a subunit of the Ca_v channels and can inhibit native calcium currents in mammalian neurons⁴¹, the TSP/ $\alpha_2\delta$ -1 pathway is thought to be at least partially independent of the roles of $\alpha_2\delta$ -1 as a Ca_v channel subunit^{7,10}. Therefore, the recombinant uncleaved $\alpha_2\delta$ -1_S variant used in this study should be suitable for the purpose of investigating TSP binding biochemically. Notably, we observed a minor band in the immunoblots of $\alpha_2\delta$ -1_S CTST at M_r ~25 kDa upon DTT treatment and detection with strep II-tag antibody (Fig. 2C, +DTT) which is most likely attributed to cleaved strep-tagged δ -1_S chain. This indicates the presence of a small fraction of the generated purified $\alpha_2\delta$ -1_S in a proteolytically cleaved form.

In addition to the $\alpha_2\delta$ -1_S variants generated, the α_2 peptide chain (α_2 NTST) was recombinantly produced in a similar way (Fig. 1B). Expression and purification of this fragment as well as analyses by SDS-PAGE and immunoblotting (Fig. 2D) were carried out as described above. Here, we observed the formation of a high molecular weight product under non-reducing conditions which dissociated into the monomeric form after DTT treatment (approximate M_r ~170 kDa, Fig. 2D) which points to the formation of interchain disulphide bonds in the absence of reducing agents (see also Discussion section below).

Notably, all recombinant proteins generated in this study that had been analysed by SDS-PAGE and Western Blot showed protein bands at remarkably higher M_r than expected from their amino acid sequences. It is known that the electrophoretic mobility of proteins can be greatly influenced by the extent of post-translational modifications (e.g. glycosylation) of the protein where the glycan chains do not bind SDS leading in many cases to decreased mobility, and increased M_r , of the glycoprotein analysed by SDS-PAGE⁴². In addition, sample treatment prior to loading onto the gel (e.g. heating at 95 °C with DTT) represents a possible source of abnormal protein migration on the gels through its impact on the structure of the analysed protein⁴³. Therefore, further analysis was carried out to determine the accurate molecular masses of the recombinant purified proteins using MALDI-TOF mass spectrometry. The results are shown in Table 1 and Supplementary Fig. S2. The molecular masses of TSP-4 and COMP, both in monomeric form, were found to be only slightly higher (1–3 kDa) than the theoretical masses calculated on the basis of each protein's amino acid sequence, indicating minor post-translational modifications,

Protein	$m/z_{\text{calc}} [M + H]^+$	$m/z_{\text{exp}} [M + H]^+$
TSP-2 (monomer)	132,137	146,958
TSP-4 (monomer)	107,409	109,351
COMP (monomer)	84,714	88,463; 87,178
$\alpha_2\delta-1_s$ NTST (-DTT)	123,000	152,236
$\alpha_2\delta-1_s$ NTST (+DTT)	112,130*	152,258

Table 1. Molecular masses of recombinant TSPs and $\alpha_2\delta-1_s$ NTST obtained by MALDI-TOF MS. The $m/z_{\text{calc}} [M + H]^+$ values for all proteins (in Da) were calculated based on their amino acid sequences using ExPASy Compute pI/Mw online tool, while the $m/z_{\text{exp}} [M + H]^+$ values (in Da) were obtained from the MALDI-TOF MS spectra of the respective proteins. * $m/z_{\text{calc}} [M + H]^+$ of α_2 NTST was calculated for the expected product of the DTT-mediated reduction of the disulphide bond between α_2 and $\delta-1_s$ in $\alpha_2\delta-1_s$ NTST.

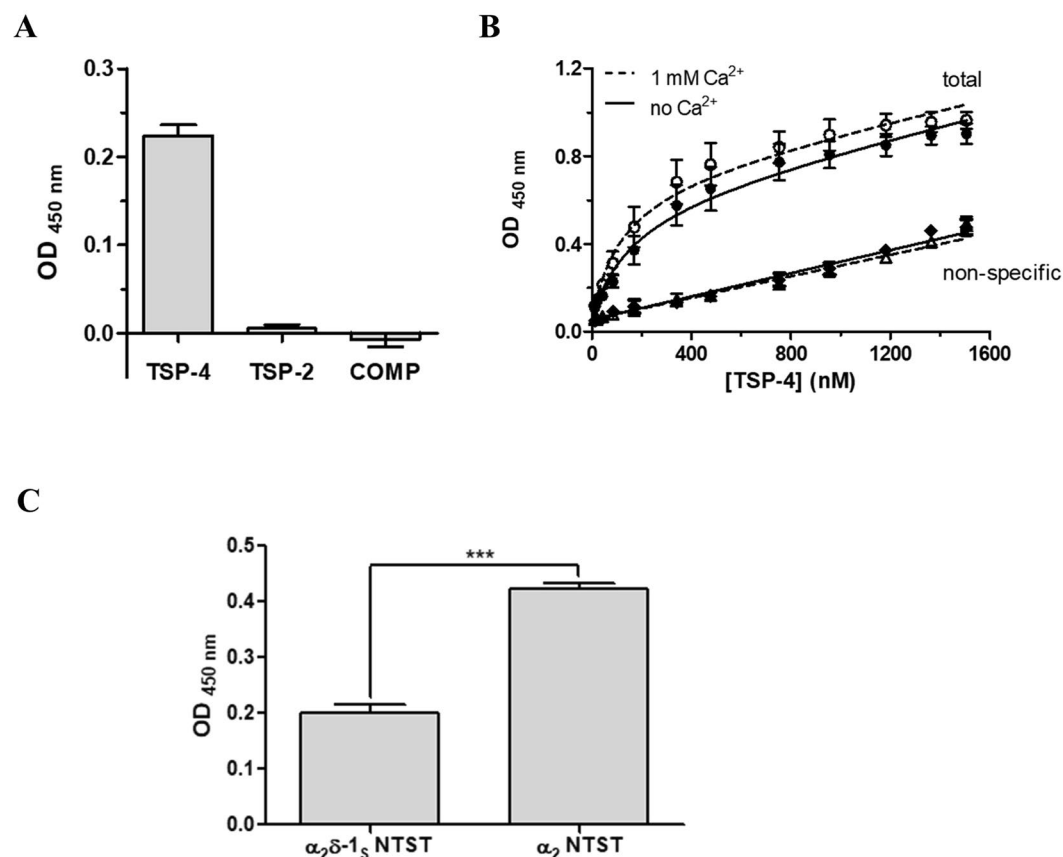


Figure 3. The direct binding to $\alpha_2\delta-1_s$ NTST is TSP-4 specific in an ELISA-style ligand binding assay. $\alpha_2\delta-1_s$ NTST (20 $\mu\text{g}/\text{ml}$) was coated onto 96-well plates and incubated with either (A) TSP-2, TSP-4 or COMP (1,000 nM), or (B) increasing concentrations of TSP-4 (11–1,505 nM). Shown are data for total (circles) and non-specific (triangles, rhombi) binding in the absence (full symbols) and presence (open symbols) of 1 mM Ca^{2+} . (C) Soluble α_2 NTST or $\alpha_2\delta-1_s$ NTST (10 $\mu\text{g}/\text{ml}$) were coated onto 96-well plates and incubated with TSP-4 (1,000 nM). Binding assays (A,C) were carried out in the presence of 1 mM Ca^{2+} and bound proteins were detected with the corresponding TSP-specific antibody/antiserum (see Supplementary Table S2). Specific binding in (A,C) was calculated by subtracting OD values of non-specific binding from those of total binding. Data of total and non-specific binding were used to calculate K_D and B_{max} in (B), with the linear dependence of the non-specific signal on the TSP-4 concentration ensuring the absence of perturbations of the assay system. Data represent mean values \pm SEM of 3 independent measurements performed in duplicates or triplicates. Statistical analysis in (C) was done using unpaired two-tailed Student's t-test (***) $P = 0.0003$.

e.g. glycosylation, of these proteins. In case of TSP-2 and $\alpha_2\delta-1_s$ NTST, the experimentally determined masses were about 15 and 30 kDa, respectively, larger than the theoretical ones, which is likely attributed to heavy glycosylation, as shown previously for $\alpha_2\delta-1$ in the work of Kadurin *et al.*⁴⁴ (Table 1, Supplementary Fig. S2a,d,e).

Characterisation of the interaction of TSPs with $\alpha_2\delta-1_s$ using an ELISA-style ligand binding assay. First, the purified recombinant full-length TSPs (soluble) were examined for their direct interaction with

Assay buffer	K_D (nM)	B_{max}
TBS	198 ± 49	0.579 ± 0.066
TBS + 1 mM Ca^{2+}	153 ± 46	0.677 ± 0.054

Table 2. Binding parameters (K_D , B_{max}) for the interaction of TSP-4 with $\alpha_2\delta$ -1_S NTST. Data represent mean values ± SEM of 3 independent experiments, each performed in duplicate. Statistical analysis by an unpaired two-tailed Student's t-test showed no significant difference for K_D (apparent dissociation constant, $P = 0.5381$) and B_{max} (maximum binding, unitless, $P = 0.3138$) obtained in the absence and presence of Ca^{2+} .

immobilised $\alpha_2\delta$ -1_S NTST in an ELISA-style ligand binding assay, that was validated using the model interaction of COMP and matrilin-3 proteins⁴⁵ (Supplementary Fig. S4). Preliminary experiments with TSP concentrations up to ~500 nM had demonstrated that out of the three TSPs generated in this study, only TSP-4 was able to directly interact with $\alpha_2\delta$ -1_S NTST (data not shown). To rule out the possibility of a very low binding affinity of TSP-2 and COMP towards $\alpha_2\delta$ -1, we finally utilised a comparably high concentration (1,000 nM) of all TSP proteins in the same ELISA which confirmed our preliminary data (Fig. 3A). Therefore, we decided to focus on the interaction of TSP-4 with $\alpha_2\delta$ -1_S and study it more in detail. Notably, we detected comparable binding signals of TSP-4 to either $\alpha_2\delta$ -1_S NTST or $\alpha_2\delta$ -1_S CTST variants in a preliminary experiment (data not shown) and hence we chose to proceed with one of the two variants, namely, $\alpha_2\delta$ -1_S NTST in our binding assays. Titration of immobilised $\alpha_2\delta$ -1_S NTST with increasing concentrations of TSP-4 (11–1,505 nM) showed saturable binding with an apparent K_D value of about 200 nM. Since Ca^{2+} binding is associated with major conformational changes and structural rearrangements of both TSPs^{46,47} and the metal ion-dependent adhesion site (MIDAS) motif of $\alpha_2\delta$ -1^{17,48}, we investigated the effect of Ca^{2+} on TSP-4/ $\alpha_2\delta$ -1_S NTST interaction. Our data show that the apparent K_D value was slightly, but not significantly, decreased in presence of 1 mM Ca^{2+} (Table 2, Fig. 3B). Similarly, the maximum binding value (B_{max} , unitless) showed a small, statistically non-significant increase in presence of 1 mM Ca^{2+} (Table 2, Fig. 3B). These results indicate that the TSP-4/ $\alpha_2\delta$ -1_S NTST interaction is not sensitive to Ca^{2+} changes. Next, the ability of TSP-4 to directly interact with the α_2 fragment of $\alpha_2\delta$ -1 was analysed. Here, we observed a two-fold, statistically significant increase in the binding signal of a single concentration of TSP-4 (1,000 nM) when using immobilised α_2 NTST instead of $\alpha_2\delta$ -1_S NTST (Fig. 3C). These results indicate the localisation of the TSP-4 binding site(s) within the α_2 region of $\alpha_2\delta$ -1 in agreement with data obtained by Eroglu *et al.*⁷. The enhanced binding signal of TSP-4 to α_2 NTST is suggestive of a more favourable conformation of α_2 NTST which is more accessible for TSP-4 binding, as compared to the non-proteolytically cleaved $\alpha_2\delta$ -1_S NTST.

To investigate the effect of the known $\alpha_2\delta$ -1 ligand GBP²⁰ on the observed TSP-4/ $\alpha_2\delta$ -1_S interaction, we checked for the ability of the recombinantly expressed mutant $\alpha_2\delta$ -1_S NTST to bind GBP with high affinity ($K_D = 219$ nM) using a label-free surface plasmon resonance (SPR) assay (Fig. 4A, Supplementary Fig. S3). Our results are in agreement with the binding data for ³H-GBP to membrane preparations of heterologously expressed human $\alpha_2\delta$ -1 (K_D range of 140–175 nM)³⁸. Various GBP concentrations (0.05–1,000 μ M) were used in the TSP-4/ $\alpha_2\delta$ -1_S NTST binding assay to interfere with this protein-protein interaction but did not show inhibitory effects (Fig. 4B). To rule out the possibility that the GBP binding pocket might not be accessible after immobilisation of $\alpha_2\delta$ -1_S NTST on the ELISA microplate, we had coated the wells with $\alpha_2\delta$ -1_S NTST after pre-incubating the protein with GBP. In addition, GBP had been supplemented to the liquid phase during blocking and incubation with TSP-4 ensuring availability of a sufficient number of GBP molecules to $\alpha_2\delta$ -1_S NTST and preventing dissociation of bound GBP during the experiment. In a further experiment, the binding of various concentrations of TSP-4 (12.5–1,000 nM) to $\alpha_2\delta$ -1_S NTST was not affected by the highest GBP concentration (1,000 μ M) investigated (Fig. 4C). Together, these data suggest that GBP alone is not sufficient to disrupt the interaction of TSP-4 with $\alpha_2\delta$ -1 on a molecular level.

Fluorescent A555-TSP-4 does not bind to membrane-bound $\alpha_2\delta$ -1 in a cell-based binding assay. To examine the interaction between TSP-4 and full-length membrane-bound $\alpha_2\delta$ -1 in a cellular environment, HEK293-EBNA cells were transfected with either empty vector or vector encoding $\alpha_2\delta$ -1 FL NTST. Immunocytochemical analysis of cells transfected with $\alpha_2\delta$ -1 FL NTST revealed a marked increase in $\alpha_2\delta$ -1 immunoreactivity, confirming the over-expression of heterologous $\alpha_2\delta$ -1 (Fig. 5A, left column).

In cells immunostained without permeabilisation, a high degree of co-localisation of $\alpha_2\delta$ -1 and wheat germ agglutinin (WGA) used for labelling glycoproteins or glycolipids of the outer leaflet of the plasma membrane⁴⁹ were observed, assuring the localisation of heterologous $\alpha_2\delta$ -1 in the plasma membrane (Fig. 5A, upper left image). The transfected cells were incubated with increasing concentrations of fluorescently labelled A555-TSP-4 (9–909 nM), the binding of which to $\alpha_2\delta$ -1_S NTST was found to be non-significantly lower than that of unlabelled TSP-4 in ELISA-style assay (Fig. 5B). Images of the stained cells were acquired using a High Content Screening microscope and the average A555-TSP-4 signal intensity was determined for each well. In addition, $\alpha_2\delta$ -1 FL NTST was visualised by immunostaining to analyse the co-localisation of A555-TSP-4 with $\alpha_2\delta$ -1 FL NTST. Results show low overall A555-TSP-4 signal intensity which increases upon increasing the concentrations of the fluorescent protein. However, no difference was observed when comparing $\alpha_2\delta$ -1 FL NTST- and empty vector-transfected cells (Fig. 5C). Furthermore, no co-localisation of A555-TSP-4 and $\alpha_2\delta$ -1 FL NTST signals was detected in these experiments (Supplementary Fig. S5). These results are in accordance with recently published data by Lana *et al.*³⁸ showing no TSP-4 co-localisation with $\alpha_2\delta$ -1 on the cell surface of tsA-201 cells co-expressing both proteins or in mixed populations of cells transfected separately with either $\alpha_2\delta$ -1 or TSP-4.

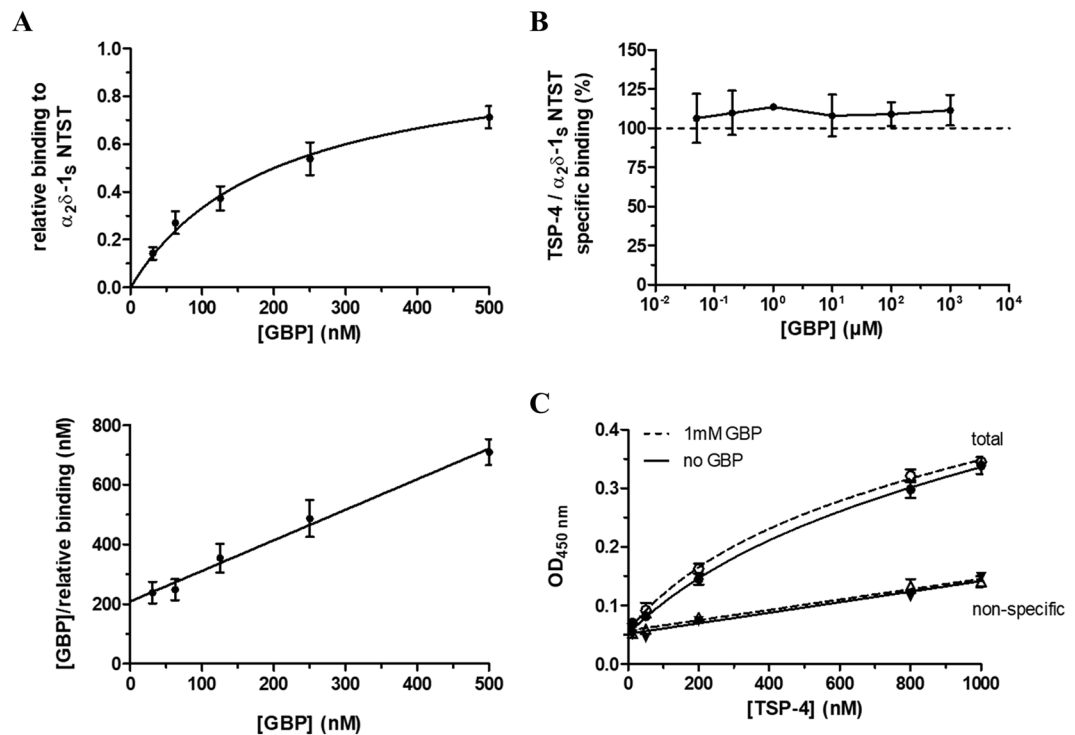


Figure 4. GBP does not directly interfere with the binding of TSP-4 to $\alpha_2\delta-1_s$ NTST in an ELISA-style ligand binding assay. (A) Surface plasmon resonance (SPR) measurements of the binding of GBP to recombinant $\alpha_2\delta-1_s$ NTST. The protein (10–15 $\mu\text{g}/\text{ml}$) was directly immobilised to CM5 sensor chips and GBP (31.25–500 nM) in PBS buffer, pH 7.4 containing 0.05% Tween 20 was passed over the chip at a flow rate of 30 $\mu\text{l}/\text{min}$. Shown are data of the relative GBP binding to $\alpha_2\delta-1_s$ NTST (Top) obtained from single cycle kinetics protocol (mean values \pm SEM of 4 independent experiments, Fig. S3). Each experiment was analysed by non-linear regression according to the equation $\text{RU}/\text{RU}_{\text{max}} = [\text{GBP}]/(K_D + [\text{GBP}])$, where the ratio of the binding response and the maximum binding response, $\text{RU}/\text{RU}_{\text{max}}$, represents the relative binding at a given GBP concentration, $[\text{GBP}]$, and K_D is the dissociation constant of the two interaction partners. Data analysis yielded a value of $K_D = 219 \pm 47$ nM (mean value \pm SEM, $n = 4$), with the linear shape of the Hanes-Woolf transformation (Bottom) showing equimolar binding of the two interaction partners. For the ELISA-style assay, the $\alpha_2\delta-1_s$ NTST (10 $\mu\text{g}/\text{ml}$) protein was coated onto 96-well plates and incubated with either (B) TSP-4 (1,000 nM) in the absence and presence of increasing concentrations of GBP (0.05–1,000 μM), or (C) increasing concentrations of TSP-4 (12.5–1,000 nM) in the absence (full symbols) and presence (open symbols) of GBP (1,000 μM). The assay was carried out in the presence of 2 mM Mg^{2+} and bound TSP-4 was detected with TSP-4-specific antiserum. Specific binding was calculated by subtracting OD values of non-specific binding (triangles) from those of total binding (circles). Data in (B) and (C) represent mean values \pm SEM of 2 to 3 independent experiments, each performed in duplicate. In (B) the OD values for specific binding of TSP-4 in the presence of GBP (0.05–1,000 μM) were normalised to those in the absence of GBP.

Discussion

All TSPs, i.e. TSPs 1–4 and COMP, were previously identified as synaptogenic proteins which, together with other astrocyte-derived factors, help to promote the formation of functional excitatory synapses in the CNS^{6,7}. The $\alpha_2\delta-1$ protein was demonstrated to be functionally involved in TSP-induced synaptogenesis by means of synaptic assays in retinal ganglion cells (RGCs)⁷, DRG/spinal cord primary neuron co-culture^{8,9}, purified cortical neurons¹⁰ as well as in dorsal spinal cord of mice³⁴. Biochemically, $\alpha_2\delta-1$ was reported to interact in co-immunoprecipitation experiments with TSP-1, TSP-2 and TSP-4 from rat cerebral cortex⁷ as well as with TSP-4 from rodent spinal cord³⁴. Similarly, a TSP-2 fragment containing all three EGF-like repeats, the calcium-binding repeats, and the C-terminal globular domain was co-purified with full-length $\alpha_2\delta-1$ or its protein-binding VWA domain after co-expression in HEK293 cells⁷. Recently, Park *et al.*^{9,34} demonstrated for the first time a direct molecular interaction between $\alpha_2\delta-1$ and recombinant full-length TSP-4 or its fragments containing EGF-like or coiled coil domains. In the present study, we investigated the biochemical properties of the direct TSP-4/ $\alpha_2\delta-1$ interaction. Furthermore, it was of importance to know whether other members of the TSP protein family are also able to directly bind to $\alpha_2\delta-1$ in an analogous manner to that of TSP-4. Our data demonstrated that only full-length TSP-4, but not TSP-2 or COMP, is able to directly interact with immobilised soluble $\alpha_2\delta-1$ variant ($\alpha_2\delta-1_s$ NTST) in an ELISA-style ligand binding assay (Fig. 3A), indicating the specificity of this protein-protein interaction. This observation is in direct contrast to that of Eroglu *et al.*⁷ (see above). Nevertheless, TSP-4 is remarkably the only isoform of TSP proteins reported so far to be implicated in neuropathic and joint-mediated chronic pain in

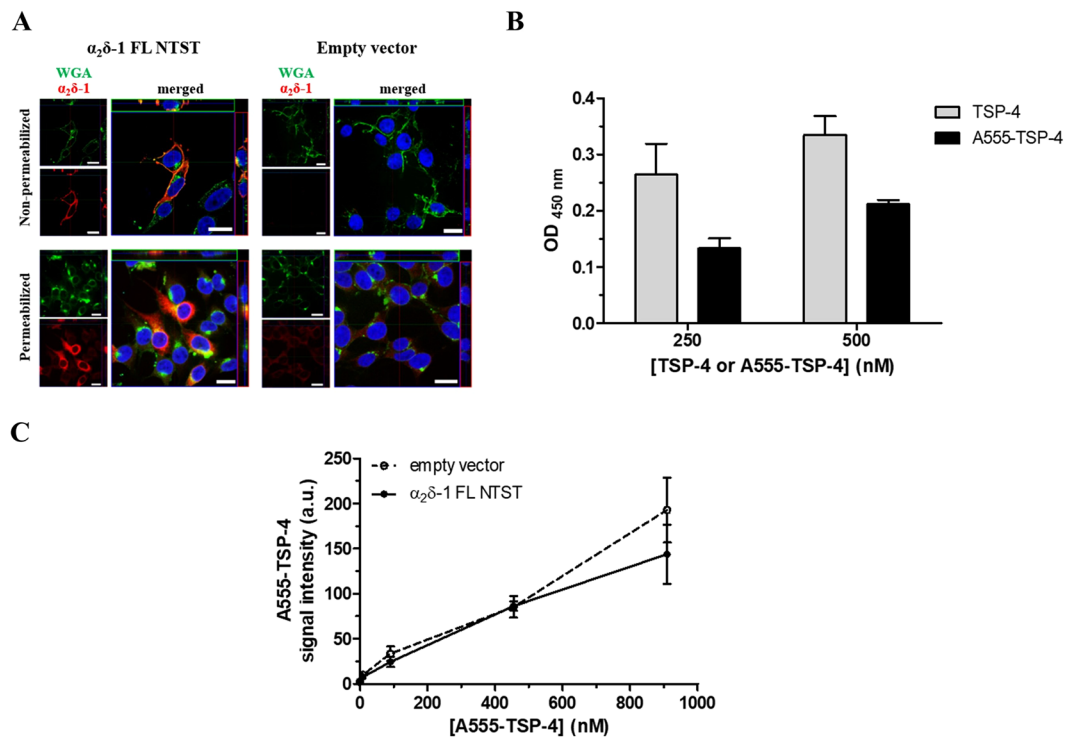


Figure 5. Fluorescent A555-TSP-4 protein does not bind to membrane-bound $\alpha_2\delta-1$ in HEK293-EBNA cells. **(A)** Representative confocal images of the immunocytochemical detection of membrane-localised $\alpha_2\delta-1$ FL NTST over-expressed in HEK293-EBNA cells. Cells were transfected with either empty vector (right column) or vector encoding full-length $\alpha_2\delta-1$ containing an N-terminal strep II-tag ($\alpha_2\delta-1$ FL NTST, left column). Cells were stained either without permeabilisation (upper row) or after membrane permeabilisation (lower row). Signals of WGA conjugated with Alexa Fluor 633 (green) and $\alpha_2\delta-1$ (red) are shown individually in the small images; merged signals are shown in the large images. DAPI was used to visualise the nucleus (blue). Images show top view as well as upper-side (green box) and right-side (red box) views of a single slice of scanning near the middle of cells. Scale bar is 20 μm for all images. **(B)** Binding of A555-TSP-4 or TSP-4 to $\alpha_2\delta-1$ NTST analysed by an ELISA-style ligand binding assay. $\alpha_2\delta-1$ NTST (20 $\mu\text{g}/\text{ml}$) was coated onto 96-well plates and incubated with either TSP-4 or A555-TSP-4 at two different concentrations (250 and 500 nM) for each protein. Specific binding was calculated by subtracting OD values of non-specific binding from those of total binding. Data represent mean \pm SEM of 2 independent measurements, each performed in duplicate. OD values for specific binding of TSP-4 and A555-TSP-4 were subjected to unpaired Student's t-test. No significant difference was found ($P > 0.05$) for each of the two concentrations of both TSP-4 species used. **(C)** Cells transfected with either empty vector or vector encoding $\alpha_2\delta-1$ FL NTST were incubated with increasing concentrations of A555-TSP-4 (final concentration: 9–909 nM) in 96-well imaging plates. Control wells received the same volume of dilution medium (40 μl) without A555-TSP-4. Average A555-TSP-4 fluorescent signal intensities from wells containing cells transfected with $\alpha_2\delta-1$ FL NTST encoding vector or empty vector (\pm SEM of 3 independent experiments, each performed in triplicate) were plotted versus the A555-TSP-4 concentration.

rodents along with neuronal $\alpha_2\delta-1$ ^{8,9,31,34,35}. During the processes resulting in such pain, both TSP-4 and $\alpha_2\delta-1$ are up-regulated on the protein level and temporally correlate with the development of behavioural hypersensitivity in the respective animal models (for review see ref.⁵⁰). In contrast, TSP-1/-2, though previously shown to be up-regulated after ischemic brain injury in rodents^{4,51} and promoting the subsequent synaptic recovery⁵¹, are not dysregulated on the protein level in dorsal spinal cord after spinal nerve ligation in mice, even when behavioural hypersensitivity was evident in these animals. This observation led Kim *et al.*³¹ to rule out the possibility of the involvement of these two astrocyte-secreted proteins in mediating TSP/ $\alpha_2\delta-1$ -induced neuropathic pain. With regards to COMP, it has been reported to be expressed in several tissues including skeletal muscle, tendon, and cartilage. In the latter tissue, COMP is known to be mainly involved in chondrocyte differentiation, attachment, and cartilage extracellular matrix assembly^{52–55}, with mutations in COMP being associated with pseudoachondroplasia^{56,57}. COMP in skeletal muscle, tendons, and perichondrium can be theoretically in contact with nerve terminals containing $\alpha_2\delta-1$. In addition, COMP was shown to have synaptogenic potential in RGCs (as discussed) and shares a high degree of both overall sequence identity (~70%) and structural similarity (Fig. 1A) with TSP-4. That is why we investigated COMP as a potential interaction partner of $\alpha_2\delta-1$ in our binding studies. Nevertheless, COMP is, in contrast to TSP-4, neither abundant in neurons and astrocytes nor it is known to be dysregulated in neuropathic pain states. The fact that, beside TSP-4, all other TSPs were previously found to induce synaptogenesis through a mechanism involving neuronal $\alpha_2\delta-1$ ⁷ may refer to other cellular factors

or scaffold proteins required to mediate their interaction with $\alpha_2\delta$ -1 indirectly. Furthermore, it is tempting to speculate that TSP-induced synaptogenesis might be of little relevance to neuropathic pain development since, as previously mentioned, TSP-4 is the only member of TSP family found to be up-regulated in dorsal spinal cord following nerve injury. Indeed, a recent study shows that an enhanced presynaptic NMDA receptor activity, rather than synaptogenesis, is responsible for maintaining the increased synaptic excitatory transmission in dorsal spinal cord leading to chronic pain states following nerve injury in mice⁵⁸.

In further experiments, we observed a significantly increased binding of TSP-4 to α_2 NTST when compared to $\alpha_2\delta$ -1_S NTST (Fig. 3C), confirming previous data by Eroglu *et al.*⁷ demonstrating the TSP-4 binding site to be localised within the α_2 region of $\alpha_2\delta$ -1 (VWA domain). The observed enhancement in binding towards α_2 might be attributed to more exposed TSP-4 binding motif(s) in the immobilised α_2 NTST compared to the non-proteolytically processed $\alpha_2\delta$ -1_S NTST. This result is in agreement with recent findings from Lana *et al.*³⁸ where wild-type $\alpha_2\delta$ -1 was very weakly co-immunoprecipitated with TSP-4, but no co-immunoprecipitation of the mutant $\alpha_2\delta$ -1 (MIDAS^{AAA}) with TSP-4 was detected in lysates of co-transfected tsA-201 cells. In addition, the binding to α_2 NTST seems again to be TSP-4-specific since negligible binding signals were detected when equimolar concentrations of either COMP or a truncated TSP-4 fragment were utilized in a pilot experiment (data not shown). Although our results are supported by reported data, we cannot rule out the possibility that the enhanced TSP-4 binding signal is due to improperly expressed α_2 NTST since unpaired cysteine residues, normally involved in the formation of disulphide bridges with other cysteine residues in the deleted regions of wild-type $\alpha_2\delta$ -1⁵⁹, become available. It is worth mentioning here that a very high tendency for multimerisation was observed for a recombinant VWA domain of $\alpha_2\delta$ -1 generated in this study (data not shown) due to the formation of intermolecular disulphide bonds. Therefore, it might be appropriate to consider the expression of α_2 and VWA fragments in which the unpaired cysteines are replaced by other isosteric residues (e.g. serine) for future binding studies.

One of the reported small molecules capable of interfering with the TSP/ $\alpha_2\delta$ -1 interaction is GBP, an approved analgesic against neuropathic pain^{60–62} and a known ligand of $\alpha_2\delta$ -1²⁰. Biochemically, co-immunoprecipitation experiments showed that the interaction between a truncated TSP-2 fragment and $\alpha_2\delta$ -1 FLAG in a co-culture of two populations of HEK293 cells was diminished in the presence of GBP⁷. In addition, as previously mentioned, TSP-4 modestly but significantly reduces the binding affinity of ³H-GBP to $\alpha_2\delta$ -1, suggesting rather an allosteric than a pure competitive mode of inhibition³⁸. Furthermore, *in vivo* data revealed the ability of GBP to block TSP-4-induced neuronal sensitisation and behavioural hypersensitivity as well as changes in Ca²⁺ currents and intracellular Ca²⁺ transients after injuries to peripheral nerves or facet-joint in rodents^{8,9,34,35,63}. Similarly, several studies in neuropathic pain models demonstrated the ability of GBP to inhibit $\alpha_2\delta$ -1-induced²⁶ or TSP-induced^{7,8,34,35} synaptogenesis. Most recently, GBP was also shown to inhibit TSP-2-induced synapse formation in purified culture of cortical neurons¹⁰. Despite the multidimensional evidence of GBP interference with TSP/ $\alpha_2\delta$ -1 interaction, a direct GBP inhibition of this interaction on the molecular level has never been investigated before, to our knowledge. In the current study, we did not observe any inhibition of the direct TSP-4/ $\alpha_2\delta$ -1_S NTST interaction in the presence of increasing concentrations (up to 1 mM) of GBP (Fig. 4B). Furthermore, the highest GBP concentration used (1 mM) did not shift the TSP-4/ $\alpha_2\delta$ -1_S NTST binding curve (Fig. 4C). Although the utilised $\alpha_2\delta$ -1_S NTST was mostly expressed as uncleaved form of the protein (in agreement with the original work describing a similar porcine $\alpha_2\delta$ -1 mutant⁴⁰), we were able to demonstrate the ability of this $\alpha_2\delta$ -1_S mutant to retain high affinity for GBP (Fig. 4A). For this purpose, a newly developed SPR-based binding assay suitable for detecting and quantifying the binding of small molecules to immobilized recombinant $\alpha_2\delta$ -1_S was used. This SPR assay has the advantage of being radiolabel-free and can easily be used to determine the binding kinetics unlike the previously used ³H-GBP binding assay^{38,40,64,65}. Taken together, our data confirmed that the proteolytic cleavage of $\alpha_2\delta$ -1 is not crucial for the formation of the GBP binding pocket⁴⁰. The complete lack of GBP inhibition towards the interaction of purified TSP-4 with $\alpha_2\delta$ -1_S NTST raises questions regarding the exact mechanism by which GBP can block the above-mentioned TSP-induced changes. It is possible that other unknown factors in the cellular environment are essential for GBP to interfere with $\alpha_2\delta$ -1/TSP-4 interaction and thereby mediating the known GBP inhibitory effects. Another possible explanation based on the recent findings of Chen *et al.*^{58,66} is that the $\alpha_2\delta$ -1/NMDA receptor complex, rather than $\alpha_2\delta$ -1/TSP-4 binding, represents the molecular target of gabapentinoid drugs to alleviate neuropathic pain.

Our efforts were as well focused on the investigation of the TSP-4/ $\alpha_2\delta$ -1 interaction in a cellular system to get closer to the physiological/pathological situation in the CNS. We over-expressed full-length $\alpha_2\delta$ -1 in HEK293-EBNA cells and demonstrated both its intracellular and plasma membrane localisation in transfected cells (Fig. 5A). Treatment with increasing concentrations (up to 909 nM) of fluorescently labelled A555-TSP-4, however, showed no differences in binding of the protein to $\alpha_2\delta$ -1 overexpressing cells when compared to control cells (Fig. 5C, Supplementary Fig. S5). Furthermore, fluorescent signals of A555-TSP-4 did not co-localise with those of immunostained $\alpha_2\delta$ -1 on the cells (Supplementary Fig. S5). The observed loss of binding cannot be attributed to an impairment of the interaction of the two proteins by the fluorescent label of TSP-4 since the fluorescent protein was generated with a minimal dye-to-protein molar ratio and showing substantial $\alpha_2\delta$ -1_S NTST binding in the ELISA-style assay (Fig. 5B). A possible explanation could instead be arising from the weak interaction of the two proteins under the conditions of the cell-based assay, unlike the ELISA-style assay. This means that very high local concentrations of TSP-4 in the proximity of cell-surface $\alpha_2\delta$ -1 would be required to enable the detection of their interaction by simulating the pathological situation (e.g. dramatic up-regulation following nerve injury). This could not, however, be achieved with the range of A555-TSP-4 concentrations (up to 909 nM) used in the assay. In our experiments, we over-expressed $\alpha_2\delta$ -1 in HEK293-EBNA cells without co-expression of α_1 subunit, which interacts intracellularly with $\alpha_2\delta$ -1 before trafficking of the complex to the cell surface⁶⁷. However, we assume that the lack of α_1 subunit did not hamper the putative binding of TSP-4 to $\alpha_2\delta$ -1 on the cell surface. This assumption is based on recent data showing the ability of wild-type $\alpha_2\delta$ -1, expressed in HEK293 cells without co-expression of α_1 subunits, to be efficiently transported to the cell surface and thereby become

accessible to extracellular ligands like TSP¹⁰. Functionally, this $\alpha_2\delta$ -1 over-expression construct alone was able to rescue synapses in cortical organotypic slices from $\alpha_2\delta$ -1 knockout mice. This effect is found to be mediated through activation of the small Rho GTPase Ras-related C3 botulinum toxin substrate 1 (Rac1) and is independent of α_1 subunits of the postsynaptic L-type calcium channels $Ca_v1.2$ and $Ca_v1.3$ ¹⁰.

The $\alpha_2\delta$ subunits are thought to promote membrane trafficking of the pore subunits of voltage-gated calcium channels¹⁷ and $\alpha_2\delta$ -1-driven allodynia in mice can be reversed by blockers of voltage-gated calcium channels like ω -conotoxin GVIA⁶⁸. However, other findings suggest that the maladaptive changes contributing to chronic pain in rodents following nerve injuries and resulting from the interaction of dysregulated TSP-4 with $\alpha_2\delta$ -1 are partially independent of the role of the latter protein in regulating voltage-gated calcium channels' trafficking and function⁵⁰.

As previously mentioned, our data align with those of Lana *et al.*³⁸ who reported no interaction of secreted TSP-4 with membrane-localised $\alpha_2\delta$ -1 on tsA-201 cells when subjected to immunocytochemical analysis. On the other hand, the same study showed weak intracellular interaction of both proteins in co-immunoprecipitation experiments from cells over-expressing both proteins³⁸. It has therefore been postulated that the weak TSP-4/ $\alpha_2\delta$ -1 interaction may occur in an intracellular compartment rather than on the cell surface^{38,69}. This postulation is in contrast to the previous data showing synaptogenic effect of secreted TSPs which is mediated by neuronal $\alpha_2\delta$ -1 thought to be located either pre-⁸ or post-^{7,10} synaptically. To our knowledge, there are no data so far showing the co-localisation of TSP(-4) and $\alpha_2\delta$ -1 in neuronal cell cultures or spinal cord tissue where TSP-induced changes (e.g. synaptogenesis) were demonstrated. To reveal the exact cellular localisation of TSP-4/ $\alpha_2\delta$ -1 interaction it would be very helpful to simultaneously analyse co-immunostained TSP-4 and $\alpha_2\delta$ -1 proteins in cultures of neurons utilized in *in vitro* synapse assays^{6,7,10}.

In summary, our results provide substantial *in vitro* biochemical evidence for a direct and specific Ca^{2+} -insensitive TSP-4/ $\alpha_2\delta$ -1 interaction which is rather weak. Importantly, GBP does not inhibit this interaction on a molecular level, indicating the possible involvement of other unknown factors or targets in mediating GBP inhibitory effects in neuropathic pain.

We, therefore, need to understand the exact and complete molecular mechanism of the TSP/ $\alpha_2\delta$ -1 interaction to really be able to design appropriate small molecule modulators - rather than being left to use and optimize the enigmatic properties of the serendipitously discovered gabapentinoid action.

Materials and Methods

Cloning, expression and purification of recombinant proteins. The plasmids encoding full-length murine TSP-2 (TSP-2, accession no. of the translated protein product [AAH53702.1](#)), full-length rat COMP (COMP, accession no. of the translated protein product [EDL90681.1](#)), and full-length rat TSP-4 (TSP-4, accession no. of the translated protein product [NP_058829.1](#)) were generated as described earlier for COMP⁷⁰. The cDNAs encoding human $\alpha_2\delta$ -1 soluble variant⁴⁰ with an N-terminal or a C-terminal double strep II-tag ($\alpha_2\delta$ -1_S NTST and $\alpha_2\delta$ -1_S CTST, respectively) and its α_2 peptide chain with an N-terminal double strep II-tag (α_2 NTST) were amplified following the same protocol from a pIRESpuro3- $\alpha_2\delta$ -1 vector, originally generated from human $\alpha_2\delta$ -1 FL cDNA⁷¹ ($\alpha_2\delta$ -1, accession no. of translated protein product [XP_005250627.1](#)). All PCR products were lacking the natural signal peptide sequences and harboured a *NheI* restriction site at the 5'-end and a *XhoI* or *BamHI* site at the 3'-end. After digestion with *NheI* and either *XhoI* or *BamHI*, the amplified cDNAs were cloned into the modified episomal expression vector pCEP-Pu-double strep II-tag (N- or C-terminal)⁷² in-frame with the 5' sequence of the BM-40 signal peptide and confirmed by Sanger nucleotide sequencing. Here, the sequences of the double strep II-tag and the thrombin cleavage site were directly located either at the 5'- or the 3'-end of the inserted cDNA sequences.

The recombinant plasmids carrying cDNAs encoding full-length proteins or truncated fragments were transfected into human embryonic kidney 293/Epstein-Barr virus nuclear antigen cells (HEK293-EBNA, Invitrogen) using TurboFect transfection reagent (Thermo Fischer Scientific). Transfected cells were cultured in DMEM medium supplemented with 10% FCS (Gibco), penicillin (1000 U/ml)/streptomycin (1000 μ g/ml), and puromycin (3 μ g/ml, Gold Biotechnology) for positive selection and were incubated at 37°C/5% CO₂ to allow growth to 100% confluency as adherent monolayers in cell culture triple-flasks (Nunc™, Thermo Fisher Scientific). Cell culture supernatants containing the secreted target proteins were collected and supplemented with phenylmethylsulfonyl fluoride (1 mM, Applichem) before passing over self-packed streptactin-sepharose columns (0.5 ml, IBA). The recombinant double strep II-tagged proteins were eluted with phosphate-buffered saline (PBS), pH 7.4 containing D-desthiobiotin (2.5 mM, Sigma), concentrated with Amicon ultra centrifugal filter units with molecular weight cutoff of 100 kDa for all recombinant proteins (Millipore), aliquoted after addition of glycerol (10% (v/v)) and stored at -80°C until use.

Coomassie stained gels and immunoblotting analysis. For protein analysis by Coomassie staining, the purified TSPs were separated on 0.5% (w/v) agarose/3% (w/v) polyacrylamide composite gels⁷³ without prior DTT treatment, while $\alpha_2\delta$ -1_S NTST and α_2 NTST variants were separated using conventional SDS-PAGE on 7% gels in presence and absence of DTT. Gels were stained overnight with colloidal Coomassie staining solution followed by destaining for 1–2 hours in a solution of ethanol (10% v/v) and o-phosphoric acid (2% v/v). All purified proteins were subjected to immunoblotting analysis by separating the proteins using SDS-PAGE under non-reducing and reducing conditions on 4–15% gradient gels for TSPs, 10% gels for $\alpha_2\delta$ -1_S NTST and $\alpha_2\delta$ -1_S CTST (before and after digestion with thrombin), and 7% gel for α_2 NTST. Proteins were then transferred onto PVDF membranes by blotting overnight at 4°C and blocked with 5% skimmed milk in Tris-buffered saline (TBS), pH 7.4 for 1 h at RT. The blocked membranes were incubated with antibodies recognizing the (double) strep II-tag or specific epitopes of the proteins for 1 h at RT, followed by incubation with the corresponding horseradish

peroxidase-conjugated secondary antibodies (see list of antibodies used in Supplementary Table S2) for 1 h at RT. Protein bands were visualised using the Odyssey Fc Imaging system (LI-COR Biosciences).

Mass spectrometry. The masses of the purified recombinant $\alpha_2\delta$ -1_S NTST and TSPs were determined by MALDI-TOF mass spectrometry performed in the bioanalytical laboratory of the Centre for Molecular Medicine Cologne (CMMC) using a similar protocol to that described by Klatt *et al.*⁷⁴. Briefly, TSPs and $\alpha_2\delta$ -1_S NTST were first incubated with DTT (10 mM) in PBS overnight at 4 °C with additional sample of $\alpha_2\delta$ -1_S NTST being treated similarly but without DTT. Next, samples were desalted with micro Zeba Spin desalting columns (Pierce Biotechnology, Thermo Fisher Scientific) equilibrated in trifluoroacetic acid (0.1% (v/v)) in ultrapure water. 5 μ l of the eluate were mixed with 5 μ l of a saturated solution of sinapinic acid (Bruker) in acetonitrile (50% (v/v)), trifluoroacetic acid (0.1% (v/v)), and 1 μ l of the mixture was applied onto a MTP 384 polished steel target (Bruker). MALDI spectra were acquired with an Ultraflextreme MALDI-TOF/TOF instrument (Bruker) operated in linear mode. The monomer ($[M + H]^+$, $[M + 2H]^{2+}$) and dimer ($[2M + H]^+$) peaks of bovine serum albumin (BSA, AppliChem) were used for external calibration of the spectra. Analysis of the MS spectra was done with FlexAnalysis software (Bruker).

Fluorescence labelling of TSP-4. TSP-4 was labelled with Alexa Fluor 555 succinimidyl ester (Life Technologies) according to manufacturer's instructions. Briefly, buffer exchange of protein samples to 100 mM NaHCO₃, 100 mM NaCl (pH 8.3) was performed using Amicon ultra centrifugal filter unit (Millipore). Protein sample was then incubated with a five-fold amount of Alexa Fluor 555 succinimidyl ester (stock dissolved at 10 mg/ml in dry dimethylformamide) for 1 h at 25 °C followed by addition of 10% (v/v) hydroxylamine (1.5 M), pH 8.5, and incubation of the hydroxylamine-containing reaction mixture for 1 h to terminate the reaction. Free dye was then separated using gel filtration by loading the protein/dye reaction mixture onto a 15-ml self-packed Sephadex G-25 (Sigma) column and elution with PBS, pH 7.4. Fractions containing labelled protein eluted in the void volume were pooled, mixed with glycerol 10% (v/v) and stored at -80 °C until use.

ELISA-style ligand binding assay. Purified $\alpha_2\delta$ -1_S NTST (10 or 20 μ g/ml) or α_2 NTST (10 μ g/ml) in coating buffer (TBS, pH 7.4 with or without 1 mM Ca²⁺ or with 2 mM Mg²⁺ for experiments with GBP) were coated overnight at RT onto 96-well plates (Nunc Maxisorb) to obtain 0.5–1 μ g protein/well for determination of values of total binding. Values of non-specific binding were obtained by adding coating buffer to the wells and proceeding similarly. After a three-cycle wash with TBS/0.05% Tween 20, pH 7.4 using a Tecan plate washer HydroFlex, wells were blocked for 2 h at RT with 5% skimmed milk in TBS, pH 7.4. Full-length TSPs and A555-TSP-4 were diluted in 5% skimmed milk in TBS, pH 7.4. TSP-4 final concentrations of either 11–1,505 nM or 12.5–1,000 nM were utilised for titration experiments in presence or absence of Ca²⁺ (1 mM) or in presence of GBP (1,000 μ M) and Mg²⁺ (2 mM), respectively, while other TSPs and A555-TSP-4 were applied at final concentrations of 250, 500 or 1,000 nM for single point determinations. All protein ligands were incubated in the corresponding wells for 2 h at RT. Experiments investigating the influence of GBP on the interaction of $\alpha_2\delta$ -1_S NTST and TSP-4 were done by adding the respective amount of GBP (Sigma-Aldrich, #G154, 100 mM stock in water, final concentration: 0.05–1,000 μ M) during coating, blocking and incubation with TSP-4. After a three-cycle wash with TBS/0.05% Tween 20, pH 7.4, bound ligands were incubated with TSP-specific antibodies followed by corresponding secondary antibodies conjugated to horseradish peroxidase (Supplementary Table S2). Quantification of bound TSPs was achieved by measuring horseradish peroxidase (HRP) activity using tetramethylbenzidine (62.5 μ g/ml, Roth) and hydrogen peroxide (0.00525% (v/v)) as substrate (50 μ l substrate solution/well). Absorbance was measured at 450 nm on a Biotek Synergy 2 multimode microplate reader with the software Gen 5 version 1.11.5 after stopping the enzymatic reaction by adding 50 μ l/well of sulfuric acid (10% (v/v)). Data of total and non-specific binding were used to calculate apparent K_D values with GraphPad Prism v5.04 for Windows (GraphPad Software, San Diego, CA, USA).

Surface Plasmon Resonance (SPR). The GBP- $\alpha_2\delta$ -1_S NTST binding experiments were carried out using BIAcore T200 and CM5 Sensor Chips (GE Healthcare) at 25 °C. The recombinant $\alpha_2\delta$ -1_S NTST protein was diluted in immobilisation buffer (sodium acetate, 10 mM, pH 5) at 10–15 μ g/ml and injected at a flow rate of 10 μ l/min for 7 min to be directly coupled to the dextran matrix of a CM5 sensor chip flow cells using amine coupling kit as described before⁷⁵. Excess reactive esters were quenched by injection of 1 M ethanolamine-hydrochloride, pH 8.5. The binding assays were performed using degassed PBS buffer, pH 7.4 containing 0.05% Tween 20 as running buffer. A serial dilution of GBP at concentrations of 31.25–500 nM was prepared in the running buffer and injected at a flow rate of 30 μ l/min over the $\alpha_2\delta$ -1_S NTST-coated and reference flow cells in a single cycle kinetics protocol. Non-specific binding signals of GBP observed in the flow cell with no immobilized protein were subtracted from all sensograms using BIAevaluation software (version 2.0, GE Healthcare Sciences). Relative binding of GBP to $\alpha_2\delta$ -1_S NTST was plotted versus the GBP concentration with equimolar interaction of the binding partners being verified by means of a Hanes-Woolf transformation. Data plotting and analysis was done with GraphPad Prism v5.04 for Windows (GraphPad Software, San Diego, CA, USA).

Immunostaining of HEK293-EBNA cells. HEK293-EBNA cells transfected with $\alpha_2\delta$ -1 FL NTST encoding vector or empty vector using Viromer Red transfection reagent (Lipocalyx) were plated in flat-bottom wells of poly-L-lysine-coated μ -slides (8-well, ibidi GmbH) and grown in appropriate DMEM medium supplemented with 3 μ g/ml puromycin for positive selection of transfected cells. The cells were incubated at 37 °C/5% CO₂ until they reached 60–70% confluency and then immunostained. Briefly, cells in all wells on the μ -slide were washed 2x with PBS, immediately fixed with 4% paraformaldehyde in PBS for 5 minutes, and subsequently washed again 2x with PBS (all done at RT). Cells were then either permeabilised by addition of 0.2% Triton X-100 in PBS for 15 min at RT or left with no permeabilization followed by a similar washing step of all cells.

To reduce non-specific staining, cells were incubated with 5% donkey serum (Sigma-Aldrich, D9663) in PBS for 60 min at RT. Subsequently, cells in all wells were incubated with anti-dihydropyridine receptor antibody (α_2 subunit, Sigma, D219), diluted at 1:100 in 1% donkey serum/PBS overnight at 4 °C, followed by incubation with donkey anti-mouse IgG-Alexa Fluor[®] 568 antibody (1:300) in 1% donkey serum/PBS containing DAPI for 1 h at RT. Next, cells were washed with PBS and incubated for 15 min with fluorescent wheat germ agglutinin (WGA)-Alexa Fluor 633 conjugate (Life Technologies, #W21404) diluted at 1:200 in PBS, for co-staining of plasma membrane. Unbound WGA was subsequently removed through a double wash step with PBS. Finally, cells were mounted in DABCO antifade solution (Carl Roth) to reduce photobleaching. Cells were examined on a confocal laser scanning microscope Zeiss LSM880 using 63 \times oil-immersion objective. The confocal optical sections were adjusted to 0.4–0.6 μ m. Images were processed using Zen 2.3 lite software and assembled using Adobe Photoshop CS5.1 v.12.0.4 (Adobe Systems Inc., San Jose, CA, USA).

Cell-based protein binding assay. HEK293-EBNA cells transfected with $\alpha_2\delta$ -1 FL NTST encoding vector or empty vector using TurboFect transfection reagent (Thermo Fischer Scientific) were suspended in DMEM cell culture medium supplemented with 10% FCS (Gibco), penicillin (1000 U/ml)/streptomycin (1000 μ g/ml), and puromycin (3 μ g/ml, Gold Biotechnology). The cells were seeded at 4,800–6,000 cells/well onto 96-well imaging plates (Greiner) after pre-coating with poly L-ornithine (0.1 mg/ml, Sigma) and were incubated overnight at 37 °C/5% CO₂ prior to the day of experiment. On the day of experiment, the cell culture medium in the wells was exchanged with 40 μ l of fluorescently labelled A555-TSP-4 in increasing concentrations (final concentration: 9–909 nM) diluted in cell culture medium. Control wells received the same volume of medium (40 μ l) without A555-TSP-4. After incubation for 1 h at RT, cells in the wells were washed 3x with cell culture medium before fixation with 4% paraformaldehyde (Sigma) in PBS for 10 min at RT. Cells were then rinsed 3x with PBS (100 μ l/well) followed by blocking for 1 h at RT with 50 μ l normal goat serum blocking buffer containing 2% goat serum (Dianova), 1% bovine serum albumin, 0.1% Triton X-100 in PBS/0.05% Tween 20. One out of three-replicate wells for both control and A555-TSP-4-treated cells were then incubated with 30 μ l of either mouse anti-dihydropyridine receptor (α_2 subunit) antibody or mouse anti-strep II-tag antibody after dilution in PBS/1% BSA at 1:500 and 1:200, respectively, while the second and third replicate wells received the same volume (30 μ l) of PBS/1% BSA without antibody. The plate was then left overnight at 4 °C. On the next day, cells were first rinsed 3x with PBS (with 10 min intervals) before addition of 50 μ l/well of donkey anti-mouse IgG-Alexa Fluor[®] 488 conjugated secondary antibody diluted at 1:1000 in PBS and containing DAPI (0.05 μ g/ml, Molecular Probes) for nuclear staining. The plate was then left in the dark for 1 h at RT followed by rinsing the cells with PBS as described before. Finally, the wells were filled with 200 μ l of PBS, sealed with aluminum sealing and stored at 4 °C until scanning. Images of the stained cells (1104 \times 1104 pixels) were acquired using a Cellomics ArrayScan XTI microscope with a light-emitting diode light source using a 20 \times objective and analysed using the Cellomics software package v.6.6.0 (Thermo Scientific Cellomics HCS Studio). Cell nuclei were identified by DAPI staining according to the object identification parameters: size, 40–800 μ m²; ratio of perimeter squared to 4 π area, 1–3; length-to-width ratio, 1–5; average intensity, 500–5000; total intensity, 2 \times 10⁵–1 \times 10⁷. The cellular region of interest was defined by extending the nuclear region by maximally 10 μ m and used to quantify fluorescence signals at desired wavelengths. Average signal intensity of A555-TSP-4 from three independent experiments was plotted against A555-TSP-4 concentrations.

Data availability

The data generated and/or analysed during the current study are available from the corresponding author on reasonable request.

Received: 31 August 2017; Accepted: 21 October 2019;

Published online: 07 November 2019

References

- Adams, J. C. Thrombospondins: multifunctional regulators of cell interactions. *Annu Rev Cell Dev Biol* **17**, 25–51 (2001).
- Adams, J. C. & Lawler, J. The thrombospondins. *Cold Spring Harb Perspect Biol* **3**, a009712 (2011).
- Bornstein, P. Thrombospondins as matricellular modulators of cell function. *J Clin Invest* **107**, 929–934 (2001).
- Lin, T. N. *et al.* Differential regulation of thrombospondin-1 and thrombospondin-2 after focal cerebral ischemia/reperfusion. *Stroke* **34**, 177–186 (2003).
- Muppala, S. *et al.* Proangiogenic Properties of Thrombospondin-4. *Arterioscler Thromb Vasc Biol* **35**, 1975–1986 (2015).
- Christopherson, K. S. *et al.* Thrombospondins are astrocyte-secreted proteins that promote CNS synaptogenesis. *Cell* **120**, 421–433 (2005).
- Eroglu, Ç. *et al.* Gabapentin receptor $\alpha\delta\delta$ -1 is a neuronal thrombospondin receptor responsible for excitatory CNS synaptogenesis. *Cell* **139**, 380–392 (2009).
- Yu, Y. P., Gong, N., Kweon, T. D., Vo, B. & Luo, Z. D. Gabapentin prevents synaptogenesis between sensory and spinal cord neurons induced by thrombospondin-4 acting on pre-synaptic Cav alpha2 delta1 subunits and involving T-type Ca(2+) channels. *Br J Pharmacol* **175**, 2348–2361 (2018).
- Park, J. F., Yu, Y. P., Gong, N., Trinh, V. N. & Luo, Z. D. The EGF-LIKE domain of thrombospondin-4 is a key determinant in the development of pain states due to increased excitatory synaptogenesis. *J Biol Chem* **293**, 16453–16463 (2018).
- Risher, W. C. *et al.* Thrombospondin receptor alpha2delta-1 promotes synaptogenesis and spinogenesis via postsynaptic Rac1. *J Cell Biol* **217**, 3747–3765 (2018).
- Ellis, S. B. *et al.* Sequence and expression of mRNAs encoding the alpha 1 and alpha 2 subunits of a DHP-sensitive calcium channel. *Science* **241**, 1661–1664 (1988).
- Klugbauer, N., Lacinova, L., Marais, E., Hobom, M. & Hofmann, F. Molecular diversity of the calcium channel alpha2delta subunit. *J Neurosci* **19**, 684–691 (1999).
- Qin, N., Yagel, S., Momplaisir, M. L., Codd, E. E. & D'Andrea, M. R. Molecular cloning and characterization of the human voltage-gated calcium channel alpha(2)delta-4 subunit. *Mol Pharmacol* **62**, 485–496 (2002).
- Bernstein, G. M. & Jones, O. T. Kinetics of internalization and degradation of N-type voltage-gated calcium channels: role of the alpha2/delta subunit. *Cell Calcium* **41**, 27–40 (2007).

15. Davies, A. *et al.* Functional biology of the alpha(2)delta subunits of voltage-gated calcium channels. *Trends Pharmacol Sci* **28**, 220–228 (2007).
16. Hoppa, M. B., Lana, B., Margas, W., Dolphin, A. C. & Ryan, T. A. alpha2delta expression sets presynaptic calcium channel abundance and release probability. *Nature* **486**, 122–125 (2012).
17. Dolphin, A. C. Calcium channel auxiliary alpha2delta and beta subunits: trafficking and one step beyond. *Nat Rev Neurosci* **13**, 542–555 (2012).
18. Davies, A. *et al.* The alpha2delta subunits of voltage-gated calcium channels form GPI-anchored proteins, a posttranslational modification essential for function. *Proc Natl Acad Sci USA* **107**, 1654–1659 (2010).
19. Klugbauer, N., Marais, E. & Hofmann, F. Calcium channel alpha2delta subunits: differential expression, function, and drug binding. *J Bioenerg Biomembr* **35**, 639–647 (2003).
20. Gee, N. S. *et al.* The novel anticonvulsant drug, gabapentin (Neurontin), binds to the alpha2delta subunit of a calcium channel. *J Biol Chem* **271**, 5768–5776 (1996).
21. Field, M. J. *et al.* Identification of the alpha2-delta-1 subunit of voltage-dependent calcium channels as a molecular target for pain mediating the analgesic actions of pregabalin. *Proc Natl Acad Sci USA* **103**, 17537–17542 (2006).
22. Bauer, C. S. *et al.* The increased trafficking of the calcium channel subunit alpha2delta-1 to presynaptic terminals in neuropathic pain is inhibited by the alpha2delta ligand pregabalin. *J Neurosci* **29**, 4076–4088 (2009).
23. Hwang, J. H. & Yaksh, T. L. Effect of subarachnoid gabapentin on tactile-evoked allodynia in a surgically induced neuropathic pain model in the rat. *Reg Anesth* **22**, 249–256 (1997).
24. Boroujerdi, A. *et al.* Calcium channel alpha-2-delta-1 protein upregulation in dorsal spinal cord mediates spinal cord injury-induced neuropathic pain states. *Pain* **152**, 649–655 (2011).
25. Li, C. Y., Song, Y. H., Higuera, E. S. & Luo, Z. D. Spinal dorsal horn calcium channel alpha2delta-1 subunit upregulation contributes to peripheral nerve injury-induced tactile allodynia. *J Neurosci* **24**, 8494–8499 (2004).
26. Li, K. W. *et al.* Calcium channel alpha2delta1 proteins mediate trigeminal neuropathic pain states associated with aberrant excitatory synaptogenesis. *J Biol Chem* **289**, 7025–7037 (2014).
27. Luo, Z. D. *et al.* Upregulation of dorsal root ganglion (alpha)2(delta) calcium channel subunit and its correlation with allodynia in spinal nerve-injured rats. *J Neurosci* **21**, 1868–1875 (2001).
28. Zhou, C. & Luo, Z. D. Electrophysiological characterization of spinal neuron sensitization by elevated calcium channel alpha-2-delta-1 subunit protein. *Eur J Pain* **18**, 649–658 (2014).
29. Zhou, C. & Luo, Z. D. Nerve injury-induced calcium channel alpha-2-delta-1 protein dysregulation leads to increased pre-synaptic excitatory input into deep dorsal horn neurons and neuropathic allodynia. *Eur J Pain* **19**, 1267–1276 (2015).
30. Li, C. Y. *et al.* Calcium channel alpha2delta1 subunit mediates spinal hyperexcitability in pain modulation. *Pain* **125**, 20–34 (2006).
31. Kim, D. S. *et al.* Thrombospondin-4 contributes to spinal sensitization and neuropathic pain states. *J Neurosci* **32**, 8977–8987 (2012).
32. Li, K. W., Kim, D. S., Zaucke, F. & Luo, Z. D. Trigeminal nerve injury-induced thrombospondin-4 up-regulation contributes to orofacial neuropathic pain states in a rat model. *Eur J Pain* **18**, 489–495 (2014).
33. Zeng, J. *et al.* Thrombospondin-4 contributes to spinal cord injury-induced changes in nociception. *Eur J Pain* **17**, 1458–1464 (2013).
34. Park, J. *et al.* Central Mechanisms Mediating Thrombospondin-4-induced Pain States. *J Biol Chem* **291**, 13335–13348 (2016).
35. Crosby, N. D. *et al.* Thrombospondin-4 and excitatory synaptogenesis promote spinal sensitization after painful mechanical joint injury. *Exp Neurol* **264**, 111–120 (2015).
36. Crosby, N. D. & Winkelstein, B. A. Spinal Astrocytic Thrombospondin-4 Induced by Excitatory Neuronal Signaling Mediates Pain After Facet Capsule Injury. *Ann Biomed Eng* **44**, 3215–3224 (2016).
37. Pan, B. *et al.* Painful nerve injury upregulates thrombospondin-4 expression in dorsal root ganglia. *J Neurosci Res* **93**, 443–453 (2015).
38. Lana, B. *et al.* Thrombospondin-4 reduces binding affinity of [(3)H]-gabapentin to calcium-channel alpha2delta-1-subunit but does not interact with alpha2delta-1 on the cell-surface when co-expressed. *Sci Rep* **6**, 24531 (2016).
39. Carlson, C. B., Lawler, J. & Mosher, D. F. Structures of thrombospondins. *Cell Mol Life Sci* **65**, 672–686 (2008).
40. Brown, J. P. & Gee, N. S. Cloning and deletion mutagenesis of the alpha2 delta calcium channel subunit from porcine cerebral cortex. Expression of a soluble form of the protein that retains [3H]gabapentin binding activity. *J Biol Chem* **273**, 25458–25465 (1998).
41. Kadurin, I. *et al.* Proteolytic maturation of alpha2delta represents a checkpoint for activation and neuronal trafficking of latent calcium channels. *Elife*, 5 (2016).
42. Hames, B. D. Gel electrophoresis of proteins: a practical approach. 3. edn, p. 32 (Oxford University Press, 1998).
43. Unal, E. S., Zhao, R., Qiu, A. & Goldman, I. D. N-linked glycosylation and its impact on the electrophoretic mobility and function of the human proton-coupled folate transporter (HsPCFT). *Biochim Biophys Acta* **1778**, 1407–1414 (2008).
44. Kadurin, I. *et al.* Calcium currents are enhanced by alpha2delta-1 lacking its membrane anchor. *J Biol Chem* **287**, 33554–33566 (2012).
45. Otten, C. *et al.* A matrilin-3 mutation associated with osteoarthritis does not affect collagen affinity but promotes the formation of wider cartilage collagen fibrils. *Hum Mutat* **31**, 254–263 (2010).
46. Misenheimer, T. M. & Mosher, D. F. Biophysical characterization of the signature domains of thrombospondin-4 and thrombospondin-2. *J Biol Chem* **280**, 41229–41235 (2005).
47. Adams, J. C. Functions of the conserved thrombospondin carboxy-terminal cassette in cell-extracellular matrix interactions and signaling. *Int J Biochem Cell Biol* **36**, 1102–1114 (2004).
48. Whittaker, C. A. & Hynes, R. O. Distribution and evolution of von Willebrand/integrin A domains: widely dispersed domains with roles in cell adhesion and elsewhere. *Mol Biol Cell* **13**, 3369–3387 (2002).
49. Chazotte, B. Labeling membrane glycoproteins or glycolipids with fluorescent wheat germ agglutinin. *Cold Spring Harbor protocols* **2011**, pdb.prot5623 (2011).
50. Gong, N., Park, J. & Luo, Z. D. Injury-induced maladaptation and dysregulation of calcium channel alpha2 delta subunit proteins and its contribution to neuropathic pain development. *Br J Pharmacol* **175**, 2231–2243 (2018).
51. Liauw, J. *et al.* Thrombospondins 1 and 2 are necessary for synaptic plasticity and functional recovery after stroke. *J Cereb Blood Flow Metab* **28**, 1722–1732 (2008).
52. DiCesare, P., Hauser, N., Lehman, D., Pasumarti, S. & Paulsson, M. Cartilage oligomeric matrix protein (COMP) is an abundant component of tendon. *FEBS Lett* **354**, 237–240 (1994).
53. DiCesare, P. E., Morgelin, M., Mann, K. & Paulsson, M. Cartilage oligomeric matrix protein and thrombospondin 1. *Purification from articular cartilage, electron microscopic structure, and chondrocyte binding*. *Eur J Biochem* **223**, 927–937 (1994).
54. Kipnes, J. R. *et al.* Molecular cloning and expression patterns of mouse cartilage oligomeric matrix protein gene. *Osteoarthritis Cartilage* **8**, 236–239 (2000).
55. Fang, C. *et al.* Molecular cloning, sequencing, and tissue and developmental expression of mouse cartilage oligomeric matrix protein (COMP). *J Orthop Res* **18**, 593–603 (2000).
56. Briggs, M. D. *et al.* Pseudoachondroplasia and multiple epiphyseal dysplasia due to mutations in the cartilage oligomeric matrix protein gene. *Nat Genet* **10**, 330–336 (1995).
57. Hecht, J. T. *et al.* Mutations in exon 17B of cartilage oligomeric matrix protein (COMP) cause pseudoachondroplasia. *Nat Genet* **10**, 325–329 (1995).
58. Chen, J. *et al.* The alpha2delta-1-NMDA Receptor Complex Is Critically Involved in Neuropathic Pain Development and Gabapentin Therapeutic Actions. *Cell Rep* **22**, 2307–2321 (2018).
59. Wu, J. *et al.* Structure of the voltage-gated calcium channel Ca(v)1.1 at 3.6 Å resolution. *Nature* **537**, 191–196 (2016).

60. Nicholson, B. Gabapentin use in neuropathic pain syndromes. *Acta Neurol Scand* **101**, 359–371 (2000).
61. Dworkin, R. H. *et al.* Pharmacologic management of neuropathic pain: evidence-based recommendations. *Pain* **132**, 237–251 (2007).
62. Rosenberg, J. M., Harrell, C., Ristic, H., Werner, R. A. & de Rosayro, A. M. The effect of gabapentin on neuropathic pain. *Clin J Pain* **13**, 251–255 (1997).
63. Pan, B. *et al.* Thrombospondin-4 divergently regulates voltage gated Ca²⁺ channel subtypes in sensory neurons after nerve injury. *Pain* **157**, 2068–2080 (2016).
64. Brown, J. P., Dissanayake, V. U., Briggs, A. R., Milic, M. R. & Gee, N. S. Isolation of the [3H]gabapentin-binding protein/alpha 2 delta Ca²⁺ channel subunit from porcine brain: development of a radioligand binding assay for alpha 2 delta subunits using [3H]leucine. *Anal Biochem* **255**, 236–243 (1998).
65. Lana, B. *et al.* Differential upregulation in DRG neurons of an alpha2delta-1 splice variant with a lower affinity for gabapentin after peripheral sensory nerve injury. *Pain* **155**, 522–533 (2014).
66. Chen, Y., Chen, S. R., Chen, H., Zhang, J. & Pan, H. L. Increased alpha2delta-1-NMDA receptor coupling potentiates glutamatergic input to spinal dorsal horn neurons in chemotherapy-induced neuropathic pain. *J Neurochem* **148**, 252–274 (2019).
67. Cassidy, J. S., Ferron, L., Kadurin, I., Pratt, W. S. & Dolphin, A. C. Functional exofacially tagged N-type calcium channels elucidate the interaction with auxiliary alpha2delta-1 subunits. *Proc Natl Acad Sci USA* **111**, 8979–8984 (2014).
68. Matthews, E. A. & Dickenson, A. H. Effects of spinally delivered N- and P-type voltage-dependent calcium channel antagonists on dorsal horn neuronal responses in a rat model of neuropathy. *Pain* **92**, 235–246 (2001).
69. Dolphin, A. C. Voltage-gated calcium channels and their auxiliary subunits: physiology and pathophysiology and pharmacology. *J Physiol* **594**, 5369–5390 (2016).
70. Hansen, U. *et al.* A secreted variant of cartilage oligomeric matrix protein carrying a chondrodysplasia-causing mutation (p.H587R) disrupts collagen fibrillogenesis. *Arthritis Rheum* **63**, 159–167 (2011).
71. Schleithoff, L., Mehrke, G., Reutlinger, B. & Lehmann-Horn, F. Genomic structure and functional expression of a human alpha(2) delta calcium channel subunit gene (CACNA2). *Genomics* **61**, 201–209 (1999).
72. Gara, S. K. *et al.* Three novel collagen VI chains with high homology to the alpha3 chain. *J Biol Chem* **283**, 10658–10670 (2008).
73. Peacock, A. C. & Dingman, C. W. Molecular weight estimation and separation of ribonucleic acid by electrophoresis in agarose-acrylamide composite gels. *Biochemistry* **7**, 668–674 (1968).
74. Klatt, A. R. *et al.* Molecular structure, processing, and tissue distribution of matrilin-4. *J Biol Chem* **276**, 17267–17275 (2001).
75. Johnsson, B., Lofas, S. & Lindquist, G. Immobilization of proteins to a carboxymethyl-dextran-modified gold surface for biospecific interaction analysis in surface plasmon resonance sensors. *Anal Biochem* **198**, 268–277 (1991).

Acknowledgements

The authors would like to deeply thank Prof. Dr. Stefan Höning (Institute for Biochemistry I, Centre for Biochemistry, Medical Faculty, University of Cologne and Center for Molecular Medicine Cologne) and Dr. Vanya Uzunova (BIAcore Application Specialist, GE Healthcare Europe) for their great help in developing the SPR-based GBP binding assay. The authors also thank Dr. Stefan Müller from the proteomic facility, Centre for Molecular Medicine Cologne for performing the MS analyses of recombinant proteins. This work was financially supported by a full PhD scholarship to Ehab El-Awaad from the German Academic Exchange Service-German Egyptian Research Long-Term Scholarship (DAAD-GERLS, code numbers: A/12/93239, 91541390) and by the Graduate Program in Pharmacology and Experimental Therapeutics (project N14) of the University of Cologne and Bayer Healthcare.

Author contributions

E.E. designed and conducted all experiments, analysed the data, interpreted the results, and wrote the manuscript. G.P. performed cell transfection, immunostaining and analysis of the respective data; C.F. cloned $\alpha_2\delta$ -1 NTST and $\alpha_2\delta$ -1 CTST constructs and participated in protein purification. J.M. contributed to the interpretation and discussion of the results. J.I. assisted in the design of the cell-based assay and in data analysis. T.H. assisted in the design of the cell-based assay and in data analysis. W.F.N. assisted in analysis of immunostaining experiments. S.H. developed the overall concept of the study. M. Paulsson developed the overall concept of the study. F.Z. developed the overall concept of the study, interpreted the experiments and wrote the manuscript. M. Pietsch developed the overall concept of the study, interpreted the experiments and wrote the manuscript. All authors participated in editing and discussing the manuscript.

Competing interests

The authors declare no competing interests.

Additional information

Supplementary information is available for this paper at <https://doi.org/10.1038/s41598-019-52655-y>.

Correspondence and requests for materials should be addressed to M.P.

Reprints and permissions information is available at www.nature.com/reprints.

Publisher's note Springer Nature remains neutral with regard to jurisdictional claims in published maps and institutional affiliations.



Open Access This article is licensed under a Creative Commons Attribution 4.0 International License, which permits use, sharing, adaptation, distribution and reproduction in any medium or format, as long as you give appropriate credit to the original author(s) and the source, provide a link to the Creative Commons license, and indicate if changes were made. The images or other third party material in this article are included in the article's Creative Commons license, unless indicated otherwise in a credit line to the material. If material is not included in the article's Creative Commons license and your intended use is not permitted by statutory regulation or exceeds the permitted use, you will need to obtain permission directly from the copyright holder. To view a copy of this license, visit <http://creativecommons.org/licenses/by/4.0/>.

© The Author(s) 2019